Collective properties of the odd-mass I nuclei: ^{123,125,127}I

R. E. Shroy,* D. M. Gordon,† M. Gai,‡ and D. B. Fossan
Department of Physics, State University of New York, Stony Brook, New York 11794

A. K. Gaigalas§
Department of Physics, State University of New York, Binghamton, New York 13901

(Received 7 April 1982)

The high-spin states of ^{123,125,127}I have been investigated via the ^{A}Sn(^{6}Li,3n)$^{A+3}$I reactions to study the collective properties of the odd-mass I isotopes. In-beam measurements of γ-ray excitations, γ-γ coincidences, γ-ray angular distributions, and pulsed beam-γ timing were performed with Ge detectors to determine level energies, decay schemes, γ-ray multipolarities, J^{π} assignments, and lifetime information. A similar study of the ^{117,119,121}I isotopes is reported in the following paper. Two collective features have been identified in these odd-mass I nuclei. Systematic $\Delta J=1$ bands built on low-lying $\frac{9}{2}^{+}$ proton-hole (4p-1h) states were observed. The $\frac{9}{2}^{+}$ bandheads, that involve the excitation of a $1g_{9/2}$ proton across the $Z=50$ shell, drop to very low energies near the middle of the neutron shell. The properties of the $\frac{9}{2}^{+}$ proton-hole states for all of the odd-mass I isotopes are presented and related to the systematic information for the proton-hole states in the entire $Z\geq 50$ transition region. Systematic $\Delta J=2$ bands built on $\frac{11}{2}^{-}$ ($1h_{11/2}$ quasiproton) states, on $\frac{7}{2}^{+}$ ($1g_{7/2}$ quasiproton) states, and on $\frac{5}{2}^{+}$ ($2d_{5/2}$ quasiproton) states were also observed. The $\Delta J=2$ band spacings generally follow the spacings of the Te-core ground-state bands with the exception of the $\frac{11}{2}^{-}$ $\Delta J=2$ bands, for which the spacings decrease significantly relative to those for the Te cores as A decreases. These systematic properties are discussed in terms of several theoretical approaches to the onset of collectivity in transitional nuclei. An isomer at 2660 keV in ^{123}I was observed to have a mean lifetime $\tau=38\pm3$ ns.

[NUCLEAR REACTIONS $^{120-124}$Sn(^{6}Li,3n)$^{123-127}$I; measured γ-γ coincidences, $\gamma(E,\theta,t)$; deduced level schemes in odd-mass $^{123-127}$I, γ multipolarities, J^{π}, $T_{1/2}$. Enriched targets, Ge(Li) detectors.]

I. INTRODUCTION

The observed collective properties of odd-proton nuclei in the $Z>50$ transition region have generated considerable theoretical interest. Systematic experimental studies of high-spin states in the odd-mass Sb ($Z=51$) (Refs. 1–3), I ($Z=53$) (Refs. 3–5), Cs ($Z=55$) (Refs. 6 and 7), and La ($Z=57$) (Ref. 3), nuclei as a function of neutron number have been carried out at Stony Brook via γ-ray measurements following heavy-ion induced reactions. These measurements covered the transition region between the odd-mass La nuclei, for which Stephens *et al.*[8] had previously observed $\Delta J=2$ bands built on $\frac{11}{2}^{-}$ states, and the $Z=50$ closed proton shell. The entire study was motivated by the fact that the rich high-spin level spectra in odd-mass nuclei have a considerable sensitivity to the variety of coexisting collective properties.

The theoretical interpretations of odd-mass transitional collectivity, involving particle (hole)-core quadrupole interactions, have traditionally approached the collectivity of the cores phenomenologically in terms of deformed rotors[9] of fixed (β,γ) coordinates or anharmonic vibrators[10] with dynamic (β,γ) coordinates. Recently the core collectivity in the $Z>50$ transition region has been examined[11] microscopically in a generalized seniority scheme with a coherent sum of core valence particles, where the microscopic particle-particle interactions gen-

erate the macroscopic particle (hole)-core interaction. The interacting boson-fermion model is also currently being explored[12] for a more detailed understanding of the collectivity of transition nuclei.

Two collective features were systematically followed in the odd-proton nuclei in the $Z > 50$ transition region.[13] Well defined $\Delta J = 2$ bands were observed on $\frac{11}{2}^-$ ($1h_{11/2}$ quasiproton) states, $\frac{7}{2}^+$ ($1g_{7/2}$ quasiproton) states, and on $\frac{5}{2}^+$ ($2d_{5/2}$ quasiproton) states in the I, Cs, and La isotopes. The $\Delta J = 2$ band spacings generally follow the spacings of the ground-state bands in the corresponding even Te, Xe, and Ba core nuclei; this feature has been interpreted with some success in terms of rotation-aligned coupling[8,9] for a modest core deformation as well as with particle (anharmonic) vibrator models.[10] A marked exception to these band spacing systematics occurs for the lower mass I nuclei where the $\frac{11}{2}^-$ $\Delta J = 2$ band spacings decrease significantly compared to the ground-state band spacings of the Te core nuclei.[4] This decrease as well as the other $\Delta J = 2$ properties can be explained in terms of a macroscopic quadrupole interaction that is generated by the number of core neutrons in an effective shell.[11]

The second collective feature of this transition region is the existence of systematic $\Delta J = 1$ bands built on low-lying $\frac{9}{2}^+$ states in the Sb, I, Cs, and La nuclei. This feature has been interpreted in terms of strongly coupled bands of a [404] $\frac{9}{2}^+$ Nilsson proton-hole orbital and a significant prolate core deformation.[2,5,14,15] Using a triaxial rotor model,[9] the Sb results imply an asymmetry of $\gamma \sim 20°$ [2]; these bands in the other isotopes seemed more consistent with symmetric rotors.[3,5,7] An anharmonic vibrator approach[10,16,17] also has been used as a basis for the $\Delta J = 1$ bands. The microscopic calculation from a generalized seniority scheme[11] was successful at achieving the low-lying $\frac{9}{2}^+$ bandhead energies as well as the band spacings. The energies of the $\frac{9}{2}^+$ bandheads, which are believed to result from the excitation of a $1g_{9/2}$ proton across the $Z = 50$ closed shell, when plotted against neutron number for each Z, follow parabolalike curves with minima near the middle of the $N = 50-82$ neutron shell. The unexpected lowering of the $\frac{9}{2}^+$ bandhead energies has been attributed to the collectivity of the core, which achieves, on the basis of the band spacings, a maximum near the middle of the neutron shell. In ^{119}Cs, the $\frac{9}{2}^+$ bandhead was surprisingly observed to have dropped in energy to become the ground state.[6,7] The $\frac{9}{2}^+$ $\Delta J = 1$ bands from Sb ($Z = 51$) to La ($Z = 57$) show a trend of decreasing band spacings with increasing Z.[13]

The complete experimental results of the odd-mass I nuclei which were obtained via (^{6}Li,$3n\gamma$) fusion-evaporation reactions are presented in this paper (I) and the following paper (II). Paper I contains the results for ^{123,125,127}I and summarizes the systematics of the $\frac{9}{2}^+$ $\Delta J = 1$ bands for all of the odd-mass I nuclei. The complete experimental results for ^{117,119,121}I are given in paper II along with a summary of the systematics of the odd-mass I $\Delta J = 2$ bands. Several preliminary reports for these nuclei have been made previously.[4,5,18]

Earlier experimental information for the odd-mass I isotopes has predominantly involved low spin states.[19] During the course of this study, some high-spin experimental information on ^{123,125}I has become available from (α,$2n$) studies.[20] Additional information on ^{117}I has also been obtained in this laboratory via the ^{106}Cd(^{11}N,$2pn$)^{117}I reaction.[3] The results of these independent experiments are in agreement with the present results, where overlap occurs. Also high-spin information was obtained in this laboratory for the next lower mass, ^{115}I, via the ^{106}Cd(^{12}C,$p\,2n$)^{115}I reaction.[3]

II. EXPERIMENTAL PROCEDURE

To study the high-spin level structure in the odd-mass $^{117-127}$I isotopes, the $\Delta Z = 3$ (^{6}Li,$3n\gamma$) fusion-evaporation reactions were used for six isotopically enriched even-Sn targets, taking advantage of the stability of the closed $Z = 50$ proton shell. The targets used in most of the measurements were either ~ 3 mg/cm^2 or 10 mg/cm^2 enriched metal foils of ^{114,116,118,120,122,124}Sn. These fusion-evaporation reactions favor population with large alignment of high spin states, whose dominant decay modes are via stretched γ-ray cascades. In order to determine the decay schemes and the level structure for the odd-mass I isotopes, the following set of γ-ray measurements using Ge(Li) and intrinsic Ge detectors was performed: γ excitation, γ-γ coincidence, γ-angular distribution, and pulsed beam-γ timing measurements. The typical energy resolution of the large volume coaxial Ge(Li) detectors was 2.2–2.5 keV FWHM at 1.33 MeV. A 5 mm thick planar intrinsic Ge detector, which was used for low energy γ rays, had an energy resolution of 0.5 keV FWHM at 122 keV. The details of the experimental techniques have been described earlier.[21,2,7]

The γ-ray excitation measurements taken over a ^{6}Li energy range from the Coulomb barrier to 35 MeV were compared with reaction calculations[22] (ALICE) as a means of selecting the optimal beam energies and identifying the specific $3n$ reaction channel. Most of the experiments were carried out in the ^{6}Li-beam energy range of 32–34 MeV. The γ-γ coincidence measurements were necessitated by the complex nature of the γ-ray spectra from these reactions. They were used to identify the γ-ray cascades and to establish the identities of the residual nuclei via the connection of unknown γ rays with those known from previous β decay or light-ion reaction studies.

To obtain information on γ-ray multipolarities and intensities I_γ, γ-ray angular distributions were measured in singles at four angles between 153° and 90°. The photopeak areas were extracted and fitted to

$$W(\theta)=I_\gamma[1+A_2P_2(\cos\theta)+A_4P_4(\cos\theta)] ,$$

where the P_n are the Legendre polynomials. Spin assignments were made on the basis of the $W(\theta)$, I_γ, and lifetime information, assuming the population of low-m substates and the decay via stretched ($J\rightarrow J-L$) transitions; these assumptions have been found empirically to be valid for the dominant γ-ray decay modes following heavy-ion fusion evaporation reactions. The mixing ratios δ for the transitions of mixed multipolarity were obtained from the tables[23] of Der Mateosian and Sunyar using the A_2 coefficients extracted from the angular distribution results.

To locate isomeric states and to study their decay modes, pulsed beam-γ measurements were performed for each of the Sn targets using a pulsed ^{6}Li beam of $\sim$2 ns width with pulse repetition periods of 1 and 4 μs. The overall time resolution obtained together with the Ge(Li) detectors was typically 3–10 ns depending upon the γ-ray energy. Delayed γ-ray energy spectra were collected for several time bins over both pulse periods, which allowed the identification of isomers by their decay transitions and yielded their approximate lifetimes. Lifetime limits were also obtained for nonisomeric states. When isomers were located, time differential spectra were then collected for selected γ-ray photopeaks to obtain precise lifetime values for the isomers. A time-differential perturbed angular distribution (TDPAD) measurement was made of the g factor for the ^{119}I isomer; this TDPAD technique will be discussed in paper II. The lifetime information including the lifetime limits obtained from these measurements further aided in the definition of specific multipolarities for the γ transitions.

III. EXPERIMENTAL RESULTS

An analysis of the singles γ-ray excitation results showed on the basis of known ground-state transitions that the (^{6}Li,$3n$) fusion-evaporation channel was dominant for the ^{120,122,124}Sn targets at 32–34 MeV. The (^{6}Li,$2n$) and (^{6}Li,$4n$) channels were observed weakly as well as those involving ^{6}Li breakup with the subsequent reactions of the α particle and the deuteron. A typical singles γ-ray spectrum for 32-MeV ^{6}Li on the ^{120}Sn target is shown in Fig. 1.

Figure 2 shows several γ-γ coincidence spectra for ^{123}I. The angular distribution information obtained for ^{123,125,127}I is given, respectively, in Tables I–III. The high-spin level structures and γ-ray decay schemes of ^{123,125,127}I deduced from these γ-ray results are shown in Figs. 3–5, respectively.

The level structures observed in the ^{123,125,127}I nuclei via the (^{6}Li,$3n$) reactions have two common collective features. The first is $\Delta J=2$ γ-ray cascades built on low-lying $\frac{11}{2}^-$, $\frac{7}{2}^+$, and $\frac{5}{2}^+$ levels. The angular distributions of the cascade members yielded A_2 and A_4 coefficients characteristic of pure $J\rightarrow J-2$ quadrupole transitions. The spacings in these cascades are fairly similar to the spacings of the corresponding even-mass Te core nuclei.

The second collective feature common to these odd-mass I nuclei is a series of $\Delta J=1$ cascades built on low-lying $\frac{9}{2}^+$ states. The angular distributions of the γ rays belonging to these cascades exhibit a mixed $M1$-$E2$ character with a positive mixing ratio δ, namely the A_2 coefficients are small because the mixed contribution for a positive δ largely cancels the negative dipole contribution. The $M1$-$E2$ character of the $\Delta J=1$ cascades is further corroborated by the observation of $J\rightarrow J-2$ $E2$ crossover transitions.

In addition to these band structures, the ^{123,125,127}I isotopes have another $\frac{9}{2}^+$ state at approximately 700 keV that decayed by dipole and quadrupole transitions, respectively, to the low-lying $\frac{7}{2}^+$ state and the $\frac{5}{2}^+$ ground state. These $\frac{9}{2}^+$ states in each case were also fed by the $\frac{11}{2}^-$ bandhead state. The spin assignments for the low-lying $\frac{5}{2}^+$, $\frac{7}{2}^+$, and $\frac{11}{2}^-$ states, which had been made in several previous studies of ^{123,125,127}I involving β decay, (^{3}He,d) reactions, and Coulomb excitation,[19] are consistent with the present measurements. The

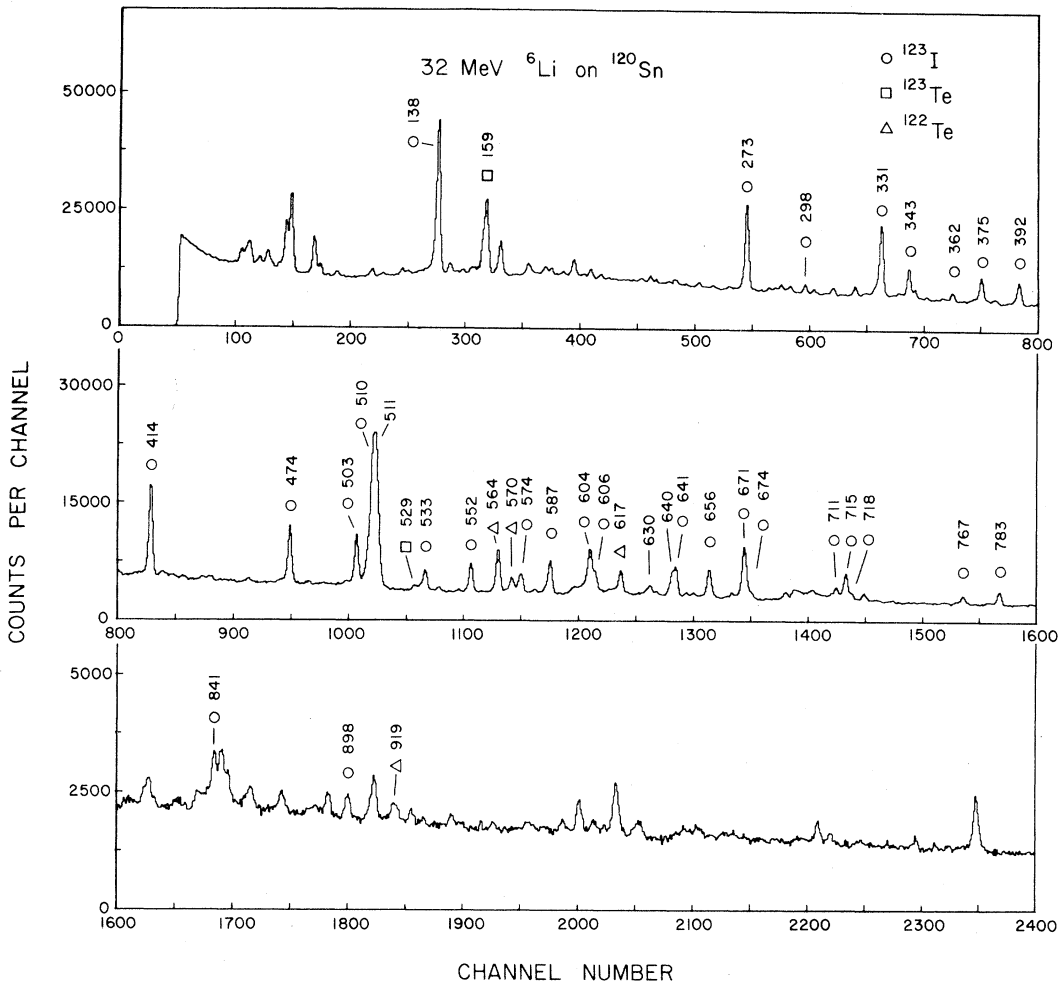

FIG. 1. γ-ray singles spectrum observed with a Ge(Li) detector for the bombardment of a ^{120}Sn target with a 32-MeV ^{6}Li beam.

overlapping information obtained for ^{123,125}I from the independent $(\alpha,2n)$ studies of Hagemann *et al.*[20] is in good agreement with the present results; the $(\alpha,2n)$ reaction achieves significant population of the nonyrast states while the present $(^{6}\text{Li},3n)$ reaction emphasizes the high-spin yrast states.

In addition to the previously discussed states in ^{127}I, a state at 3351 keV was observed to feed the $\frac{23}{2}^{-}$ member of the $\frac{11}{2}^{-}$ band. The weak intensity of the decay γ ray from this state did not allow sufficient angular distribution information to achieve a spin assignment. Also, the γ-ray deexcitating the $\frac{9}{2}^{+}$ bandhead of the $\Delta J=1$ band shown in Fig. 5 was not observed. This results from the weak population of this $\Delta J=1$ band and the low detection efficiency at the expected high γ-ray energy ($\gtrsim$1200 keV). The assignment of this $\Delta J=1$ band to the $\frac{9}{2}^{+}$ bandhead in ^{127}I is based on the systematics observed for the $\frac{9}{2}^{+}$ $\Delta J=1$ bands in $^{117-125}$I and the fact that the excitation functions of these γ rays are appropriate to ^{127}I.

The pulsed beam-γ measurements for the ^{123,125,127}I nuclei revealed no delayed γ rays except for the decay of an isomeric state located at 2660 keV in ^{123}I. This implies an upper mean-lifetime limit of $\tau\lesssim 10$ ns for all other states observed in ^{123,125,127}I (see Figs. 3–5). The weakly populated ^{123}I isomer was observed to decay via a 298.2 and 671.2 keV γ-ray cascade through a state at 2362 keV into the $\frac{15}{2}^{+}$ member of the $\frac{9}{2}^{+}$ $\Delta J=1$ band. Fits of the time differential spectra for the 298.2, 671.2, and 503.1 keV γ rays yielded a mean lifetime of $\tau=38\pm3$ ns for the 2660 keV isomer in ^{123}I. The

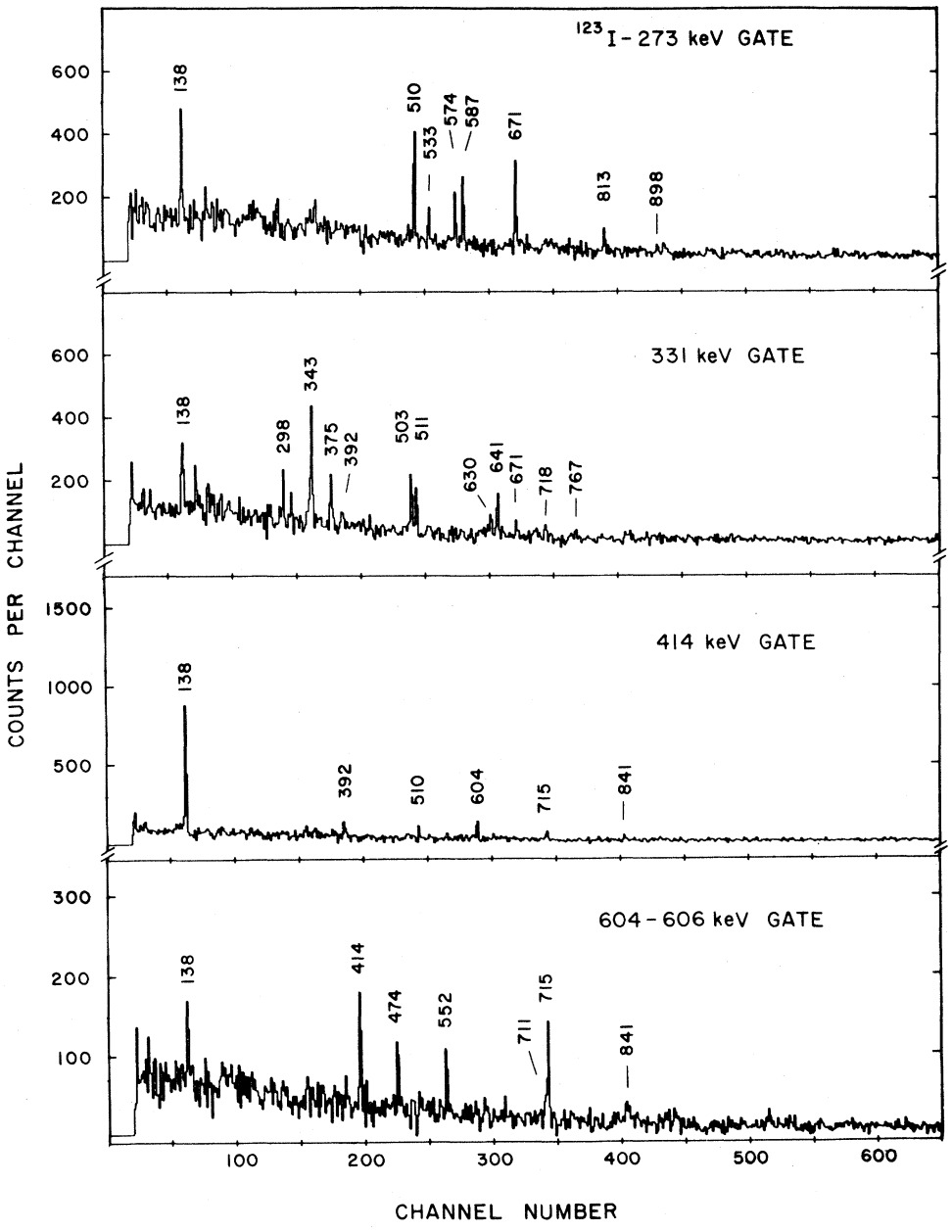

FIG. 2. Representative γ-γ coincidence spectra from the ^{120}Sn (^{6}Li,3n)^{123}I reaction for selected γ-ray gates.

(α,2n) study of ^{123}I by Hagemann *et al.*[20] resulted in a value of $\tau = 40 \pm 3$ ns for this isomer; they gave a tentative J^{π} assignment of $(\frac{21}{2}^{+})$ and $(\frac{19}{2}^{+})$ for the 2660 keV isomer and the 2362 keV level, respectively, based on electron conversion information. Two additional levels of lower spin were defined in the (α,2n) study[20] by γ rays (doublets) that were in coincidence with the isomeric decay. This is not inconsistent with the present data because of the weak population of these states by the (^{6}Li,3n) reaction.

IV. DISCUSSION

Two collective features were systematically observed in the odd-mass I nuclei studied in this work (papers I and II): (1) $\Delta J = 1$ bands built on low-

TABLE I. Angular distribution results for ^{123}I.

E_γ[a] (keV)	I_γ[b]	A_2	A_4	Branching ratio (B.R.) (%)[c]	$J_i^\pi \rightarrow J_f^\pi$	$\delta(E2/M1)$[d]
138.4	102	−0.25±0.10			$\frac{7}{2}^+ \rightarrow \frac{5}{2}^+$	−0.15±0.05
272.6	100	−0.16±0.03	−0.03±0.03	78±5	$\frac{11}{2}^- \rightarrow \frac{9}{2}^+$	
298.2	11	0.24±0.12	0.06±0.16			
331.2	117	0.12±0.04	−0.01±0.04		$\frac{11}{2}^+ \rightarrow \frac{9}{2}^+$	+0.25±0.04
343.2	45	0.06±0.03	0.00±0.03	73±5	$\frac{13}{2}^+ \rightarrow \frac{11}{2}^+$	+0.20±0.03
362.3	10	−0.73±0.09	−0.03±0.12	10±5	$\frac{13}{2}^+ \rightarrow \frac{11}{2}^+$	−0.43±0.10
375.0	47	0.00±0.04	−0.06±0.04	80±5	$\frac{15}{2}^+ \rightarrow \frac{13}{2}^+$	+0.15±0.03
391.5[e]	43	−0.08±0.03	0.01±0.04	22±5	$\frac{11}{2}^- \rightarrow \frac{9}{2}^+$	
				61±15	$\frac{17}{2}^+ \rightarrow \frac{15}{2}^+$	
414.0	89	−0.49±0.03	−0.03±0.03	61±5	$\frac{9}{2}^+ \rightarrow \frac{7}{2}^+$	−0.40±0.10
474.3[f]	59	−0.50±0.03	−0.03±0.03		$(\frac{7}{2}^+ \rightarrow \frac{5}{2}^+)$	$-0.50 < \delta < -1.20$
503.1	64	−0.46±0.06	0.00±0.07	53±5	$\frac{9}{2}^+ \rightarrow \frac{7}{2}^+$	−0.33±0.10
510±1					$\frac{15}{2}^- \rightarrow \frac{11}{2}^-$	
532.6	31	−0.25±0.04	0.09±0.05	23±5	$\frac{9}{2}^+ \rightarrow \frac{7}{2}^+$	
552.4	51	0.33±0.05	−0.05±0.06	39±5	$\frac{9}{2}^+ \rightarrow \frac{5}{2}^+$	
574.1	41	0.28±0.08	−0.06±0.10		$\frac{23}{2}^- \rightarrow \frac{19}{2}^-$	
586.8	63	0.34±0.04	−0.06±0.05		$\frac{19}{2}^- \rightarrow \frac{15}{2}^-$	
604.1	86	0.30±0.05	−0.02±0.05	90±5	$\frac{13}{2}^+ \rightarrow \frac{9}{2}^+$	
606.2[f]	36	0.24±0.04	−0.03±0.05		$(\frac{11}{2}^+ \rightarrow \frac{7}{2}^+)$	
641.3	58	0.28±0.06	−0.05±0.06	47±5	$\frac{9}{2}^+ \rightarrow \frac{5}{2}^+$	
655.9	69	0.32±0.03	−0.04±0.04		$\frac{11}{2}^+ \rightarrow \frac{7}{2}^+$	
671.2[e]	126	0.16±0.04	−0.03±0.04	77±5	$\frac{9}{2}^+ \rightarrow \frac{5}{2}^+$	
674.3	17	0.16±0.10	−0.03±0.13	27±5	$\frac{13}{2}^+ \rightarrow \frac{9}{2}^+$	
711.3[f]	25	0.38±0.05	−0.04±0.07		$(\frac{15}{2}^+ \rightarrow \frac{11}{2}^+)$	
715.4	65	0.34±0.04	−0.07±0.04		$\frac{17}{2}^+ \rightarrow \frac{13}{2}^+$	
718.1	12	0.28±0.10	0.03±0.13	20±5	$\frac{15}{2}^+ \rightarrow \frac{11}{2}^+$	
766.6	24	0.37±0.06	−0.10±0.08	39±15	$\frac{17}{2}^+ \rightarrow \frac{13}{2}^+$	
782.5	38	0.29±0.04	−0.10±0.05		$\frac{15}{2}^+ \rightarrow \frac{11}{2}^+$	
840.6	35	0.24±0.05	−0.09±0.06		$\frac{21}{2}^+ \rightarrow \frac{17}{2}^+$	
898.3	14	0.18±0.09	−0.14±0.12		$\frac{27}{2}^- \rightarrow \frac{23}{2}^-$	

[a]Energies are accurate to within ±0.3 keV unless otherwise noted.

[b]I_γ, the relative intensities, have been normalized to a strong low-lying transition; typical uncertainties are ±10% except where noted.

[c]B.R. are the branching ratios of transitions from a given initial state.

[d]The $\delta(E2/M1)$ mixing ratios were extracted from the angular distribution results following Ref. 23. An average value of the m-substate population half-width, $\sigma = 2.2 \pm 0.3$, which was obtained from pure multipolarities for the (^{6}Li,3n) reaction in this region, was assumed.

[e]Doublet unresolved in the singles spectrum; evidence from coincidence data.

[f]Not definitely placed in the decay scheme.

TABLE II. Angular distribution results for ^{125}I.

E_γ (keV)[a]	I_γ[b]	A_2	A_4	$J_i^\pi \rightarrow J_f^\pi$	Branching ratios (B.R.) (%)[c]	$\delta(E2/M1)$[d]
113.5±0.2	160±20	−0.24±0.10		$\frac{7}{2}^+ \rightarrow \frac{5}{2}^+$		
333.5±0.5	11±3	−0.05±0.03	0.02±0.08	$\frac{11}{2}^+ \rightarrow \frac{9}{2}^+$		0.11±0.05
346.2±0.5	8±2	−0.06±0.04	−0.01±0.05	$\frac{13}{2}^+ \rightarrow \frac{11}{2}^+$		0.12±0.05
380.3±0.5[e]	100	−0.18±0.04		$\frac{11}{2}^- \rightarrow \frac{9}{2}^+$		
				$\frac{15}{2}^+ \rightarrow \frac{13}{2}^+$		
435.8	25	−0.63±0.03	−0.04±0.05	$\frac{13}{2}^+ \rightarrow \frac{11}{2}^+$	32±4	0.33±0.08
481.9	62	−0.54±0.05	0.01±0.06	$\frac{9}{2}^+ \rightarrow \frac{7}{2}^+$	75±3	$-0.4 > \delta > -2.0$
505.0±0.4	21	0.17±0.04	−0.02±0.05	$\frac{23}{2}^- \rightarrow \frac{19}{2}^-$		
579.3±0.4	51	0.27±0.03	−0.04±0.06	$\frac{15}{2}^- \rightarrow \frac{11}{2}^-$		
590.7±0.4	14	0.11±0.05	0.12±0.10	$\frac{9}{2}^+ \rightarrow \frac{7}{2}^+$	14±2	0.28±0.08
595.5±0.4	21	0.20±0.06	0.03±0.07	$\frac{9}{2}^+ \rightarrow \frac{5}{2}^+$	25±3	
608.3	54	0.22±0.04	−0.05±0.04	$\frac{13}{2}^+ \rightarrow \frac{9}{2}^+$	68±4	
613.7	32	0.24±0.05	−0.03±0.08	$\frac{19}{2}^- \rightarrow \frac{15}{2}^-$		
654.4	70	0.28±0.04	−0.06±0.04	$\frac{11}{2}^+ \rightarrow \frac{7}{2}^+$		
683.7	52	0.22±0.04	−0.05±0.05	$\frac{17}{2}^+ \rightarrow \frac{13}{2}^+$		
704.2	83	0.23±0.05	0.01±0.06	$\frac{9}{2}^+ \rightarrow \frac{5}{2}^+$	86±2	
786.1	34	0.19±0.08	0.02±0.05	$\frac{15}{2}^+ \rightarrow \frac{11}{2}^+$		
822.5	19	0.04±0.05	−0.07±0.09	$\frac{9}{2}^+ \rightarrow \frac{7}{2}^+$		0.20±0.07
850.6	29	0.20±0.08	−0.06±0.09	$\frac{21}{2}^+ \rightarrow \frac{17}{2}^+$		
890±1.0	9±3	0.30±0.09	−0.08±0.07	$\frac{27}{2}^- \rightarrow \frac{23}{2}^-$		

[a]Energies are accurate to within ±0.3 keV unless otherwise noted.

[b]I_γ, the relative intensities, have been normalized to a strong low-lying transition; typical uncertainties are ±10% except where noted.

[c]B.R. are the branching ratios of transitions from a given initial state.

[d]The $\delta(E2/M1)$ mixing ratios were extracted from the angular distribution results following Ref. 23. An average value of the m-substrate population half-width $\sigma = 2.2 \pm 0.3$, which was obtained from pure multipolarities for the (^{6}Li,3n) reaction in this region, was assumed.

[e]Doublet unresolved in the singles spectrum; evidence from coincidence data.

lying $\frac{9}{2}^+$ states, and (2) $\Delta J = 2$ bands built on $\frac{11}{2}^-$, $\frac{7}{2}^+$, and $\frac{5}{2}^+$ states. A summary and discussion of all of the $\frac{9}{2}^+$ $\Delta J = 1$ bands are presented in this paper (I) while those for the $\Delta J = 2$ bands will be given in the following paper (II). The $\frac{9}{2}^+$ $\Delta J = 1$ bands observed for the odd-mass $^{117-127}$I nuclei are compared in Fig. 6; the recent work[3] on ^{117}I from this laboratory has been included in the comparison for completeness. The numbers below the $\frac{9}{2}^+$ bandheads in Fig. 6 are the excitation energies in keV. There is clearly a striking similarity in terms of the $\Delta J = 1$ band spacings, which become the smallest at ^{119}I. The excitation energies of the $\frac{9}{2}^+$ bandheads, following a parabolic shape, reach a minimum of 307 keV at ^{119}I ($N = 66$). These $\Delta J = 1$ $\frac{9}{2}^+$ band systematics for the odd-mass I ($Z = 53$) nuclei and those observed in the odd-mass Sb ($Z = 51$), Cs ($Z = 55$), and La ($Z = 57$) nuclei[13] (Fig. 7 shows the $N = 68$ isotones) suggest a collective structure that is common to this $Z \gtrsim 50$ transition region.

These $\frac{9}{2}^+$ bandheads are believed to involve the excitation of a $lg_{9/2}$ proton across the $Z = 50$ closed proton shell achieving 2p-1h states in the odd-mass

TABLE III. Angular distribution results for ^{127}I.

E_γ (keV)[a]	I_γ[b]	A_2	A_4	$J_i^\pi \rightarrow J_f^\pi$	Branching ratio (B.R.)[c]	$\delta(E2/M1)$[d]
57.6±0.2				$\frac{7}{2}^+ \rightarrow \frac{5}{2}^+$		
325.6±1.0				$(\frac{11}{2}^+) \rightarrow (\frac{9}{2}^+)$		
340.1±0.4	8±2			$(\frac{15}{2}^+) \rightarrow (\frac{13}{2}^+)$	80±10	
374.5±0.5	4±2					
396.5±0.4	8±2			$(\frac{13}{2}^+) \rightarrow (\frac{11}{2}^+)$	80±10	
430.0±0.4	7±2	0.17±0.12	−0.20±0.13	$\frac{23}{2}^- \rightarrow \frac{19}{2}^-$		
490.6	27	−0.12±0.07		$\frac{11}{2}^- \rightarrow \frac{9}{2}^+$		
550.1	32	−0.70±0.06	−0.07±0.09	$\frac{13}{2}^+ \rightarrow \frac{11}{2}^+$	62± 4	−0.40±0.15
593.4	17	−0.57±0.07	0.14±0.10	$\frac{9}{2}^+ \rightarrow \frac{7}{2}^+$		$-0.4 > \delta > -1.5$
610.1±0.4	21	0.36±0.09	0.02±0.10	$\frac{17}{2}^+ \rightarrow \frac{13}{2}^+$		
615.5	20	0.27±0.10	−0.08±0.13	$\frac{13}{2}^+ \rightarrow \frac{9}{2}^+$	38± 4	
651.8±1.0[e]	9±2	0.32±0.13	−0.19±0.17	$\frac{19}{2}^- \rightarrow \frac{15}{2}^-$		
				$\frac{9}{2}^+ \rightarrow \frac{5}{2}^+$		
658.9±1.0[e]	100	0.26±0.07	−0.05±0.09	$\frac{15}{2}^- \rightarrow \frac{11}{2}^-$		
				$\frac{11}{2}^+ \rightarrow \frac{7}{2}^+$		
686.8±0.5	8±2	0.13±0.12	−0.06±0.10	$\frac{9}{2}^+ \rightarrow \frac{7}{2}^+$	19± 6	0.30±0.20
722 ±1.0	2±1			$(\frac{13}{2}^+) \rightarrow (\frac{9}{2}^+)$	20±10	
736 ±1.0	2±1			$(\frac{15}{2}^+) \rightarrow (\frac{11}{2}^+)$	20±10	
744.8	34	0.19±0.11	−0.11±0.09	$\frac{9}{2}^+ \rightarrow \frac{5}{2}^+$	81± 6	
763.5	68	0.24±0.06	−0.08±0.09	$\frac{15}{2}^+ \rightarrow \frac{11}{2}^+$		
880.1±0.5	21	0.21±0.09	−0.13±0.11	$\frac{19}{2}^+ \rightarrow \frac{15}{2}^+$		
933.5±0.5	14	0.19±0.11	0.11±0.14	$\frac{21}{2}^+ \rightarrow \frac{17}{2}^+$		

[a]Energies are accurate to within ±0.3 keV unless otherwise noted.
[b]I_γ, the relative intensities, have been normalized to a strong low-lying transition; typical uncertainties are ±10% except where noted.
[c]B.R. are the branching ratios of transitions from a given initial state.
[d]The $\delta(E2/M1)$ mixing ratios were extracted from the angular distribution results following Ref. 23. An average value of the m-substate population half-width, $\sigma = 2.2 \pm 0.3$, which was obtained from pure multipolarities for the (^{6}Li,3n) reaction in this region, was assumed.
[e]Doublet unresolved in the singles spectrum; evidence from coincidence data.

Sb nuclei, 4p-1h states in the I nuclei, 6p-1h states in the Cs nuclei, and 8p-1h states in the La nuclei. The theoretical interpretation of the $\Delta J = 1$ collective bands can be approached macroscopically with particle (hole)-core coupling for either deformed rotors[8,9] or anharmonic vibrators.[10] Although each theoretical model can achieve somewhat equivalent results, the deformed rotor basis is a natural starting point in view of the collective properties observed for these $\frac{9}{2}^+$ $\Delta J = 1$ bands.

A strongly coupled deformed (prolate) rotor interpretation of these $\frac{9}{2}^+$ $\Delta J = 1$ bands is consistent with the observed band spacings, the positive $E2/M1$ $\Delta J = 1$ mixing ratios, the direct-to-crossover intensity ratios, and the $\frac{9}{2}^+$ bandhead energies. An axially symmetric rotor calculation[5] involving the [404] $\frac{9}{2}^+$ Nilsson proton-hole orbital, which is related to the $lg_{9/2}$ spherical orbital, has been made to interpret the $\Delta J = 1$ $\frac{9}{2}^+$ bands observed in the odd-mass I nuclei. The band-mixing

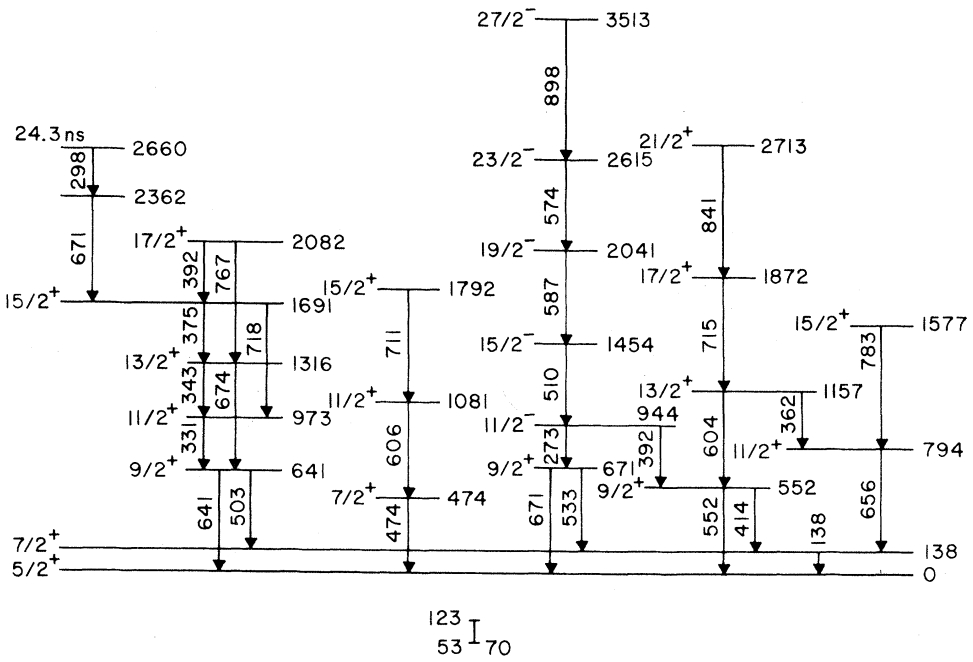

FIG. 3. Level scheme for ^{123}I extracted from the present work. All energies are in keV. The 2660 keV level is an isomer with a half-life $t_{1/2}=24.3\pm2.0$ ns.

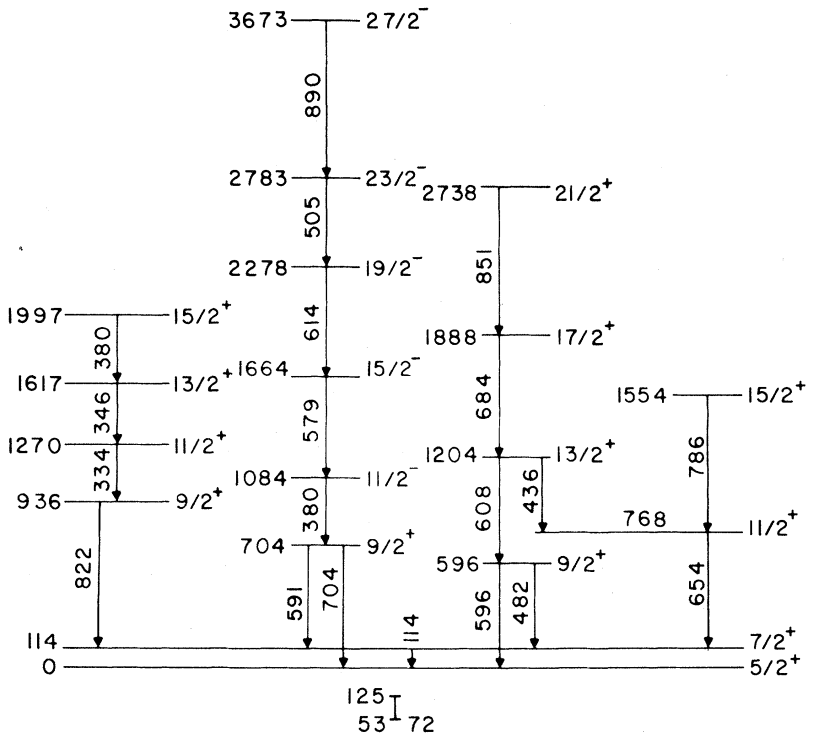

FIG. 4. Level scheme for ^{125}I extracted from the present work. All energies are in keV.

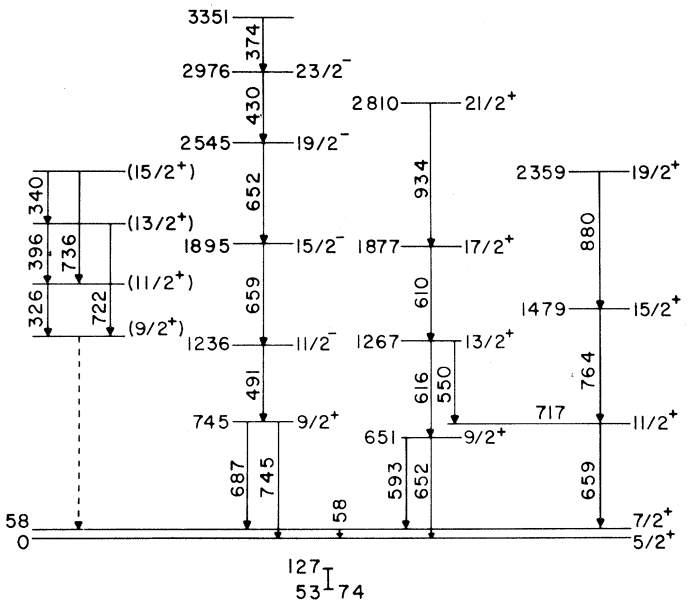

FIG. 5. Level scheme for ^{127}I extracted from the present work. All energies are in keV.

type calculations were made at the equilibrium prolate deformations which were deduced from the total potential energy surfaces for each nucleus. Reasonable agreement was achieved for the $\frac{9}{2}^+$ bandhead energies and the band energy spacings as a function of the neutron number N as shown in Figs. 4 and 5 of Ref. 5. A somewhat unsatisfying aspect of this rotor calculation is that the [404] $\frac{9}{2}^+$ amplitude of the band members decreases as J increases. For the $J^\pi = \frac{19}{2}^+$ band member of ^{121}I, for example, the [413] $\frac{7}{2}^+$ component was greater than 15%.

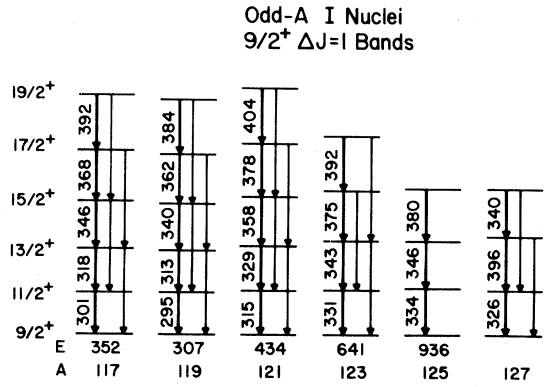

FIG. 6. Systematic properties of the observed $\Delta J = 1$ band built on the low-lying $\frac{9}{2}^+$ states in odd-mass $^{117-127}$I nuclei. The results for ^{117}I include work from Ref. 3. The γ ray and bandhead energies are in keV.

Calculations with a triaxial rotor model[9] also could achieve agreement with the $\frac{9}{2}^+$ $\Delta J = 1$ band spacings of the I nuclei for an asymmetric parameter γ near 0° (a symmetric prolate rotor). The squeezing of the $\frac{11}{2}^+$ and $\frac{13}{2}^+$ ($j+1$ and $J+2$) band members, which was observed in the Sb $\frac{9}{2}^+$ $\Delta J = 1$ bands and fitted with $\gamma = 20°$,[2] is not present in the I nuclei.

The other macroscopic approach,[10] involving the proton-hole coupled to an anharmonic-vibrator core, has been compared to the rotor-core calculations by van Isacher *et al.*[16] for the $\Delta J = 1$ $\frac{9}{2}^+$ bands in both the odd-mass Sb and I nuclei. They found fits to the band properties with sufficient anharmonic phonons that were essentially indistinguishable from those of the rotor calculation. This similarity was also extended[16] to the electromagnetic properties, which have been carefully compared for ^{115}Sb by Bron *et al.*[17] The mathematical overlap of these two macroscopic approaches prevents a definite identification of a rotor or vibratorlike basis (or possible combination) for these collective properties.

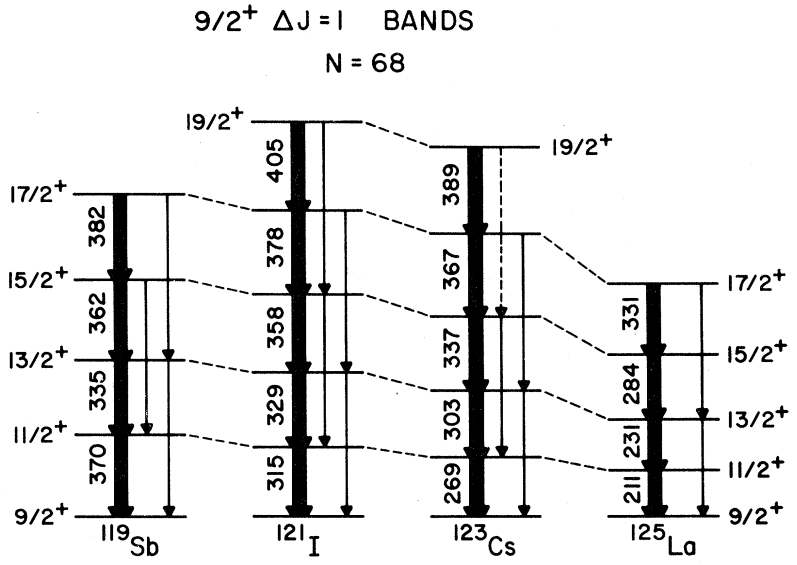

FIG. 7. Systematic $\Delta J=1$ band properties for the $\frac{9}{2}^+$ proton-hole states in the $N=68$ isotones, ^{119}Sb (Ref. 2), ^{121}I, ^{123}Cs (Ref. 7), and ^{125}La (Ref. 3). The γ-ray energies are in keV.

The nonuniqueness and approximate basis of these macroscopic approaches to the collectivity of this region provide a motivation for a more microscopic interpretation. In this respect, a microscopic generalized seniority scheme has been applied to the description of the $\frac{9}{2}^+$ $\Delta J=1$ bands observed in the $Z>50$ transition region.[11] A perturbation expansion of the particle (hole)-collective core interaction in terms of the number of neutrons in an effective shell has been obtained from a coherent sum of nucleon-nucleon interactions. A second order (seniority breaking) term introduces a quadratic dependence of the $\frac{9}{2}^+$ bandhead energies on the neutron number N. A comparison of the experimental and calculated $\frac{9}{2}^+$ bandhead energies as a function of N for the Sb and I nuclei is presented in Fig. 8. The parabolic dependence, which is obvious in the figure, has a behavior similar to that achieved by the introduction of a residual macroscopic quadrupole interaction. The experimental $\frac{9}{2}^+$ energies at $N=64$ (^{117}I and ^{115}Sb) are slightly higher than that expected from the experimental systematics or the theoretical curves; this possibly represents an influence of the subshell closure at $N=64$, which is related to the $Z=64$ closure at ^{146}Gd. The $\frac{9}{2}^+$ $\Delta J=1$ band spacings for the $Z>50$ region are also well fit in this microscopic model.[24] The resulting hole-core interaction yields weak-coupling like spin multiplets, which relate to the coupling of the odd proton-hole $J_\pi{}^{-1}=\frac{9}{2}$ to the even-Xe core J_c. The $J_{\max}$ state for each multiplet with $J_c=0, 2, 4, \ldots$ is pushed above the $J_{\max}{}^{-1}$ member by the usual particle-hole interaction resulting in $\Delta J=1$ bands. These calculations are being made[24] for the entire

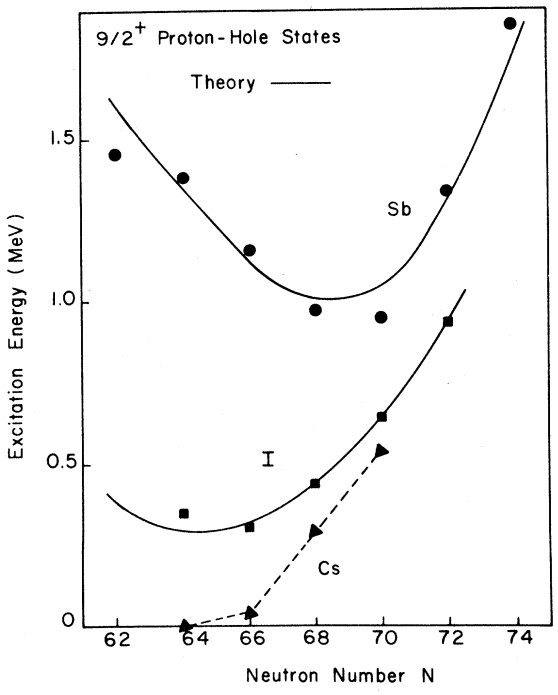

FIG. 8. Comparison of the observed $\frac{9}{2}^+$ bandhead energies for the odd-proton nuclei in the $Z>50$ transition region with microscopic calculations of Gai *et al.* (Ref. 11).

$Z > 50$ transition region. Further comparisons with this model are given in the following paper (II).

The extensive systematic experimental properties obtained for the collectivity of this $Z > 50$ transition region[13] provide a very detailed testing ground for the various microscopic theoretical approaches. It is hoped that such tests will reveal a unique understanding of this collectivity as well as that for other transition regions. Recent investigations[12] involving the interacting boson-fermion model for odd-mass nuclei are currently being directed at transition nuclei.

This work was supported in part by the National Science Foundation.

---

*Present address: Machlett Laboratories, 1063 Hope Street, Stamford, CT 06907.

†Present address: Brookhaven National Laboratory, Upton, NY 11973.

‡Present address: A. W. Wright Nuclear Structure Laboratory, Yale University, New Haven, CT 06511.

§Present address: National Bureau of Standards, FM 105, Washington, D. C. 20234.

[1]A. K. Gaigalas, R. E. Shroy, G. Schatz, and D. B. Fossan, Phys. Rev. Lett. 35, 555 (1975).

[2]R. E. Shroy, A. K. Gaigalas, G. Schatz, and D. B. Fossan, Phys. Rev. C 19, 1324 (1979).

[3]P. Chowdhury, U. Garg, A. Neskakis, W. F. Piel, Jr., T. P. Sjoreen, P. M. Stwertka, and D. B. Fossan (unpublished).

[4]D. M. Gordon, M. Gai, A. K. Gaigalas, R. E. Shroy, and D. B. Fossan Phys. Lett. 67B, 161 (1977).

[5]D. B. Fossan, M. Gai, A. K. Gaigalas, D. M. Gordon, R. E. Shroy, K. Heyde, M. Waroquier, H. Vincx, and P. Van Isacker, Phys. Rev. C 15, 1732 (1977).

[6]U. Garg, T. P. Sjoreen, and D. B. Fossan, Phys. Rev. Lett. 40, 831 (1978).

[7]U. Garg, T. P. Sjoreen, and D. B. Fossan, Phys. Rev. C 19, 207 (1979); 19, 217 (1979).

[8]F. S. Stephens, D. M. Diamond, R. M. Leigh, T. Kammuri, and K. Nakai, Phys. Rev. Lett. 29, 438 (1972).

[9]F. S. Stephens, Rev. Mod. Phys. 47, 43 (1975); J. Meyer-ter-Vehn, Nucl. Phys. A249, 111 (1975); A249, 141 (1975); H. Toki and A. Faessler, *ibid.* A253, 231 (1975).

[10]U. Hagemann and F. Donau, Phys. Lett. 59B, 321 (1975); G. Alaga and V. Paar, *ibid.* 61B, 129 (1976).

[11]M. Gai, A. Arima, and D. Strottman, Phys. Lett. 106B, 6 (1981); (unpublished).

[12]F. Iachello and O. Scholten, Phys. Rev. Lett. 43, 679 (1979); M. A. Cunningham, Phys. Lett. 106B, 11 (1981).

[13]D. B. Fossan, *Structure of Medium Heavy Nuclei, Rhodes, 1979* (Institute of Physics, Bristol, 1980), p. 151.

[14]W. D. Fromm, H. F. Brinckmann, F. Donau, C. Heiser, F. R. May, V. V. Pashkevitch, and H. Rotter, Nucl. Phys. A243, 9 (1975).

[15]K. Heyde, M. Waroquier, H. Vincx, and P. Van Isacher, Phys. Lett. 64B, 135 (1976).

[16]P. Van Isacher, M. Waroquier, H. Vincx, and K. Heyde, Nucl. Phys. A292, 125 (1977).

[17]J. Bron, W. H. A. Hesselink, H. Bedt, H. Verheal, and G. VandenBerghe, Nucl. Phys. A279, 365 (1977).

[18]D. M. Gordon, M. Gai, R. E. Shroy, D. B. Fossan, and A. K. Gaigalas, Bull. Am. Phys. Soc. 20, 1187 (1975); 20, 1188 (1975); 21, 96 (1976); 21, 634 (1976).

[19]*Tables of Isotopes,* 7th ed., edited by C. M. Lederer and V. S. Shirley (Wiley, New York, 1978); *Nuclear Level Schemes A=45 through A=257 from Nuclear Data Sheets,* edited by the Nuclear Data Group (Academic, New York, 1973); A. Szanto de Toledo, M. N. Rao, N. Ueta, and O. Sala, Phys. Rev. C 15, 238 (1977); J. R. Lien, J. Gard, C. Lunde Nilsen, and G. Lovhoiden, Nucl. Phys. A281, 443 (1977).

[20]U. Hagemann, H.-J. Keller, and H.-F. Brinckmann, Nucl. Phys. A289, 292 (1977).

[21]See, for example, B. A. Brown, P. M. S. Lesser, and D. B. Fossan, Phys. Rev. C 13, 1900 (1976).

[22]M. Blann, U. S. Atomic Energy Commission Report No. 000-3494-29 (unpublished).

[23]E. Der Mateosian and A. W. Sunyar, At. Data. Nucl. Data Tables 13, 391 (1974); 13, 407 (1974).

[24]M. Gai, A. Arima, and D. Strottman, *in Proceedings of the International Conference on Band Structure, New Orleans, 1980,* edited by A. L. Goodman (North-Holland, Amsterdam, 1980), p. 158; and (unpublished).